NOTATION

a, thermal diffusivity; λ, thermal conductivity; k, filtration coefficient; ℓ, characteristic size in the frozen zone; V, velocity; p, pressure; t, temperature; r, radius of the freezing column; Γ, surface of the freezing column; n, outer normal to ∂D_1; X and Y, Cartesian coordinates; ε, maximum transverse size of the ice–rock body. The dimensionless parameters, variables, and functions are: x, y, Cartesian coordinates; $z = x + iy$, complex variable of the physical plane; K_c, ratio of the volume heat capacities of water and soil; Pe, Peclet number; $\mu(\xi)$, heat-flux density; θ and θ_1, temperatures in the regions D and D_1, respectively; Q, intensity of the freezing column; $K_0(\xi)$, Bessel function. The indices are: T, thawed zone; M, frozen zone; c, surface of the freezing column; p, surface of the phase transition; ∞, value at infinity; *, maximum size of the ice–rock body; and, $\wedge$ designates dimensional variables.

LITERATURE CITED

1. K. G. Kornev and V. A. Chugunov, PMM, 52, NO. 6, 991-996 (1988).
2. V. L. Rvachev, PMM, 50, No. 2, 248-255 (1956).
3. A. Yu. Khasanova and G. G. Tumashev, Izv. Vyssh. Uchebn. Zaved., Mat., No. 6, 109-116 (1978).
4. V. M. Aleksandrov and E. V. Kovalenko, Problems in the Mechanics of Continuous Media with Mixed Boundary Conditions [in Russian], Moscow (1986).
5. F. D. Gakhov, Boundary-Value Problems [in Russian], Moscow (1977).
6. V. A. Chugunov and K. G. Kornev, Inzh.-fiz. Zh., 51, No. 2, 305-311 (1986).
7. L. van Wijngaarden, Proc. Koninkl. Nederl. Akad. Wet., Ser. B, 69, No. 2, 263-276 (1966).
8. V. A. Maksimov, Izv. Akad. Nauk SSSR, Mekh., No. 4, 41-45 (1965).
9. L. B. Prozorov, Freezing of Rocks during Drilling of Bore Holes [in Russian], Moscow (1961), pp. 133-193.

STUDY OF THE CHARACTERISTICS OF HEAT AND MASS TRANSFER IN A GAS–SOLID BODY SYSTEM AT LOW TEMPERATURES

N. V. Atapina, D. N. Garipogly, A. S. Drobyshev, V. A. Kuz'min, and S. L. Maksimov

UDC 542.8;620.191.5

An experimental apparatus – a universal vacuum spectrophotometer – is described. It is used for studying the kinetic characteristics of gas–solid phase transitions at low temperatures as well as the spectral reflectances of typical optical surfaces coated with layers of cryocondensates of different gases. A method is proposed for determining the indices of refraction of the cryocondensates, the growth rates of the condensates, and the spectral reflectances.

Heat and mass transfer in cryogenic–vacuum systems in the presence of gas–solid phase transitions, while obeying general laws, nonetheless exhibits a number of important peculiarities which require special study. We are referring primarily to the presence of heat and mass fluxes which are determined by the transformation of gas into a solid phase and which can be determined in the systems studied. In addition, under certain conditions, namely, high vacuum and low temperatures, the radiation component makes an important contribution to the overall heat transfer. However, the appearance of layers of cryogenically deposited gases on the heat-transfer surfaces can significantly affect the reflectances of the surfaces and the parameters of the radiation heat transfer as a whole. Since there are no thoroughly developed methods for calculating heat and mass fluxes under these conditions, it is necessary to perform experimental investigations in this direction. It should be noted that interest in such investigations has increased substantially in the last 20 years. They are, however, of a fragmentary and particularly applied character. Here, first, we call attention to [1-3],

S. M. Kirov Kazakh State University, Alma-Ata.

Translated from Inzhenerno-Fizicheskii Zhurnal, Vol. 61, No. 6, pp. 986-992, December, 1991. Original article submitted April 17, 1991.

0022-0841/91/6106-1524 $12.50

where the dependences of the spectral and integral reflectances of surfaces coated with layers of croygenic deposits of CO_2 and H_2O were studied. In [4], in addition, a model is proposed for the scattering of radiation within a layer of solidified gas. However, it was not the purpose of these investigations to make a detailed and systematic study of the dependence of the optical properties of cryocondensates on the thermodynamic parameters of the phase transition, though, obviously, and the authors of the works mentioned above point this out, the structure of the layers formed is determined significantly by the temperature of the condensation surface, which is an important characteristic. As concerns investigations of the kinetic characteristics of the transformation of gas into a solid phase, here information is even more sparse and is mostly of technical value, though the fact that there is no even somewhat completed theory of cryocondensation of gas makes this direction of investigation exceedingly interesting and necessary.

This formulation of the problem of combined study of the basic laws governing heat and mass transfer in thermodynamic systems with phase transformations requires a universal experimental apparatus with extensive possibilities for obtaining information. In our opinion, the apparatus described below meets these requirements.

Experimental Apparatus. Figure 1 shows a diagram of the experimental apparatus — a universal vacuum spectrophotometer — for performing combined investigations of the dynamics of a gas–solid phase transition and the properties of cryocondensates. The main working parameters of the apparatus are as follows:

working pressure in the chamber 10^{-6}-10^5 Pa;

temperature interval on the substrate surface 20-400 K;

spectral range of measured optical properties 0.2-20.0 μm;

measurement of the mass composition of the gas phase — up to 140 amu;

range of angles of incidence and reflection ±90°.

The main unit of the apparatus is the vacuum chamber (Fig. 1), which is connected with the injection and evacuation systems and systems for analysis of the gas phase. The chamber housing is a 430-mm diameter and 420-mm high stainless steel (Kh18N10T) cylinder. Photometric spheres with absorbing and scattering surfaces, depending on the problem at hand, can be installed in the chamber.

A cryostat (continuous-flow type) is placed at the center of the vacuum chamber. The top end of the cryostat is polished and serves as a substrate (the diameter of the working surface of the cryostat is equal to 40 mm). The cryostat also has an attachment for securing specimens. A heat exchanger with a channel of the spiral of Archimedes type to allow passage of liquid nitrogen and a heating agent is pressed into the body of the substrate. A guard ring, whose temperature is stablized independently, is provided in order to eliminate radial temperature gradients along the surface of the substrate.

The temperature of the substrate surface is measured with a three-junction copper–constantan thermocouple, and the temperature of the guard ring is measured with a four-junction thermocouple. The temperature regime is set and the substrate temperature is monitored automatically during the experiment with the help of an IVK-20 instrumentation computer.

In order to perform investigations below 80 K a microcryogenic machine (MCM), which operates at temperatures up to 20 K and has a working surface with a diameter of 80 mm, is mounted at the location of the cryostat. In this case the surfaces studied are secured on the top flange of the MCM.

The working spectral ranges in the region from 0.2 to 5.0 μm are separated with an MDR-12 monochromator and from 2.0 to 20.0 μm with an IKS-29 spectrometer. An RTN-31G converter is used to record radiation from 2.0 to 5.0 μm. The signal from the radiation detectors is measured with a universal Shch-31 voltmeter, whose digital output is connected to the IVK-20 system through an FK-73 input–output register of a CAMAC system. The IVK-20 system maintains the gas phase at the required pressure.

The program package Mono, developed in our laboratory, was employed when performing the experiments.

Experimental Procedure. Before the experiments are started, the sample, which consists of a 40-mm diameter and 20-mm thick disk, is placed on the working surface of the cryostat and is secured with the help of a special clamping device, after which the chamber cover is

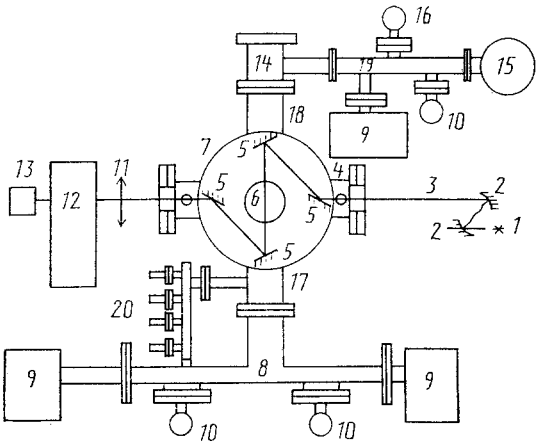

Fig. 1. Diagram of the experimental apparatus (top view): 1) radiation source; 2) parabolic mirrors; 3) radiation flux; 4) chamber window; 5) mirror lightguides; 6) cryostat; 7) chamber housing; 8) vacuum line; 9) magnetic-discharge pumps; 10) zeolite pumps; 11) condenser; 12) monochromator; 13) radiation detector; 14) air lock; 15) ROMS-2 mass spectrometer; 16) IPDO-2 mass spectrometer; 17, 18) connecting sleeve; 19) mass-spectrometric unit; 20) infiltration system.

closed and is vacuum sealed through a copper liner. Preliminary evacuation of the chamber is performed with zeolite pumps 10 (Fig. 1) to a pressure of $5 \cdot 10^{-1}$ Pa. When this pressure is reached the zeolite pumps are disengaged and further evacuation is performed with high-vacuum pumps of the type NORD-250. These operations are performed in parallel in the mass-spectrometric unit 19. When the working vacuum is reached (~$8 \cdot 10^{-6}$ Pa), the spectrum of the residual gases in the chamber is measured with the help of an IPDO-2 omegatron partial-pressure meter or an ROMS-2 mass spectrometer.

Next, the surface being investigated is cooled to the temperature of the experiment. When the latter temperature is reached the spectrum of the radiation reflected from the clean cold surface of the sample is measured. The cleanliness of the sample is checked with the help of a laser interferometer during the cooling process. Then gas is injected through a system of flow regulators 20 up to a working pressure of 10^{-3}-10^{-4} Pa. The partial pressure of the gas is then recorded with the help of the IPDO-2 pressure meter.

When gas starts to condense on the surface under study, growth-induced interference occurs and is recorded with the KSP-4 automatic plotter of the laser interferometer and the interferometer of the measuring system. When the required thickness of the cryocondensate layer is reached the flow of gas into the chamber is stopped and the spectral reflectance of the surface under study with the cryolayer is measured.

Measurement and Calculation of the Spectral Reflectances. The reflectance is measured by the relative method, which makes it possible to neglect the properties of the apparatus (window transmittances, lightguide reflectances, etc.). The spectral composition of the incident radiation, i.e., the base spectrum, is determined first. The radiation from the source 1, concentrated by a system of parabolic mirrors 2, enters the chamber through a fluorite window 4, and is guided out of the chamber with the help of the lightguides 5 (bypassing the substrate of the cryostat) and is focused with a condenser 11 on the input slit of the monochromator. The lightguides in this case are placed in the ±90° position. In order to measure the spectral composition of the reflected radiation the lightguides are placed in a prescribed position. The spectral reflectance is calculated as the ratio of the intensity of the radiation reflected from the surface under study to the intensity of the incident radiation with the same wavelength.

Measurement and Calculation of the Condenation Rate and the Thickness and Density of the Gas Cryocondensate. The quite well-known method of [5] is based on the interference of the laser radiation reflected from the surface of the substrate and from the cryocondensate–vacuum interface. We employed a helium–neon laser with wavelength $\lambda = 0.63$ μm. Using the interferogram obtained in the process of growth of the cryocondensate, i.e., knowing the or-

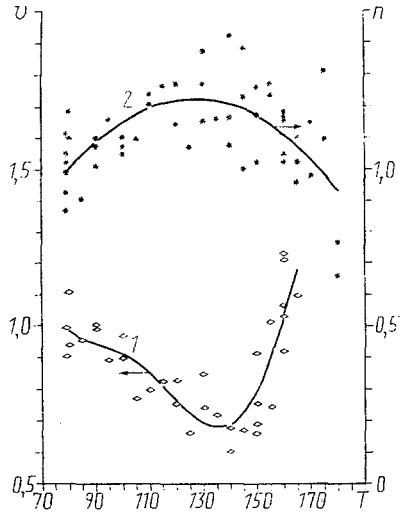

Fig. 2

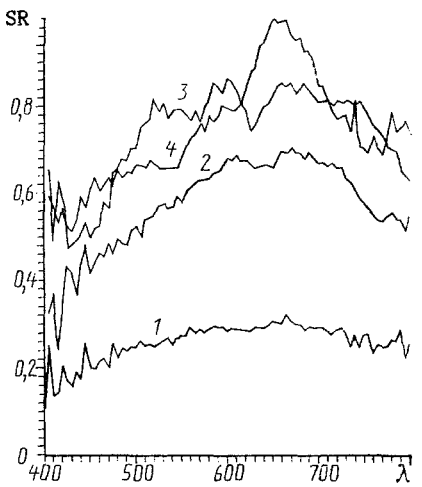

Fig. 3

Fig. 2. Reduced condensation rate (curve 1) and index of refraction (curve 2) as a function of the temperature of the condensation surface. T, K.

Fig. 3. Reduced spectral reflectance of the absorbing surface coated with layers of water cryocondensate of different thickness as a function of the wavelength of the incident radiation (nm): 1) clean surface; 2) r = 5.7 μm; 3) r = 11.7 μm; 4) r = 13.0 μm.

der of interference m, the index of refraction of the cryocondensate n, the angle of incidence of the radiation α, and the wavelength of the incident radiation λ, the thickness r of the condensate can be determined from the formula [6]

$$r = \frac{m\lambda}{2n(1 - \sin^2\psi/n^2)^{1/2}},$$

whence the condensation rate is determined as

$$v = \frac{\Delta r}{\Delta t} = \frac{m\lambda}{2n\Delta t(1 - \sin^2\psi/n^2)^{1/2}}.$$

This formula expresses the linear rate of growth of the thickness of the cryocondensate. In order to determine the condensation mass flux (kg/(m^2·sec)) it is necessary to know the density ρ of the cryocondensate formed. Since the density of the layers formed can depend significantly on the thermodynamic parameters of the phase transition, the experimental apparatus described above makes it possible to measure it directly. For this, the substrate with the cryocondensate layer of known thickness is separated in a vacuum-tight manner, with the help of a special valve, from the general volume of the chamber, after which the cryostat is heated. Once the pressure of the gas phase in the separated volume has been measured and knowing its value, the mass of the cryocondensate and its density can be calculated from the well-known formulas

$$M = \frac{PV\mu}{RT}; \quad \rho = \frac{M}{rS},$$

where S is the area of the substrate.

The correctness of these formulas is justified by the fact that the pressure of the sublimated gas in the separated volume does not exceed 30 kPa.

Calculation of the Index of Refraction of the Cryocondensate Gas. The index of refraction is calculated with the help of the double-beam method, described in detail in [7]. The index of refraction of the cryocondensates was calculated using the formula

$$n = \frac{\Delta t_1^2 \sin^2\alpha_1 - \Delta t_2^2 \sin^2\alpha_2}{\Delta t_1^2 - \Delta t_2^2},$$

where Δt_1 and Δt_2 are the interference periods for two known angles of incidence of the radiation.

Measurement Results. We present below the results of measurements of the dependence of the condensation rate, the index of refraction, and the spectral reflectance of condensates of water vapor on the temperature of the surface of condensation and the pressure of the gas phase. A mirror, made of Kh18N10T steel, and an absorbing surface were employed as the substrates. The measurements were performed in the temperature interval 79-200 K and pressure range 10^{-2}-10^{-5} Pa.

Data on the temperature dependence of the condensation rate and index of refraction of water vapor cryocondensates are presented in Fig. 2. The data are normalized to their values at T = 79 K. The curve 1 describes the dependence of the water vapor condensation rate on the substrate temperature at a pressure of $P = 5.3 \cdot 10^{-4}$ Pa. Curve 2 is a collection of values of the indices of refraction of the cryocondensate layers formed at given temperatures in the pressure range $5 \cdot 10^{-4}$-$8 \cdot 10^{-3}$ Pa. As one can see, in both cases the dependence of the measured parameters on the temperature of the gas–solid phase transition surface is strongly nonlinear.

The obtained data can be interpreted in terms of a change in the mechanism of condensation and, as a consequence, formation of phases with different structures. The possibility of such an effect was pointed out in [8], and similar temperature dependence of the condensation rate was observed previously in [9] for a number of gases. In [9] it was suggested that the observed effect occurs when the mechanism of condensation of the gas–metastable liquid–crytal is replaced by a mechanism that is less favorable energetically, but becomes the thermodynamically preferable gas–crystal mechanism as the substrate temperature decreases. Apparently, the results studied in the present paper can be explained quite accurately on the basis of the assumptions made above, especially since everyone knows that both supercooled water and water extended with respect to pressure at the triple point are present.

The effect of cryocondensate layers of water vapor of different thickness on the mirror spectral reflectance of different surfaces is shown in Figs. 3 and 4. Thus, Fig. 3 shows the wavelength dependence of the spectral reflectance of an absorbing surface for different thicknesses of water vapor cryocondensates, formed at T = 120 K and $P = 10^{-4}$ Pa. The results are normalized to the maximum spectral reflectance for a clean surface. Obviously, as the thickness of the cryocondensate increases the spectral reflectance of the surface increases significantly in the entire wavelength range.

Data on the wavelength dependence of the spectral reflectance of a metallic mirror in the near-IR region are presented in Fig. 4 for different thicknesses of water vapor cryocondensates. These results are also normalized to the maximum spectral reflectance for a clean surafce. The dependences presented show that quite thin condensate layers radically change the behavior of the spectral reflectance of the surface under study. A sharp maximum appears in the region of 3-μm radiation. This peak is obviously the resonance line of molecular absorption by layers of condensed water. As the thickness of the deposit increases the absorption peak broadens in the direction of long wavelengths, and the spectral reflectance of the surface decreases.

CONCLUSIONS

1. The experimental apparatus described in this paper makes it possible to perform extensive investigations of heat and mass transfer in cryogenic–vacuum systems and to obtain reliable results.

2. Kinetic data were obtained during water vapor condensation on the cooled substrate. These results combined with the data obtained on the dependence of the index of refraction of a cryodeposit layer on the condensation conditions allows us to conclude that the mechanism of the gas–solid phase transition changes in the region studied.

3. It was shown that the formation of cryocondensate layers results in a sharp change of the spectral reflectances of both absorbing and reflecting surfaces. Calculations of the radiation heat transfer parameters performed neglecting this effect give a strongly distorted description of the processes that actually occur.

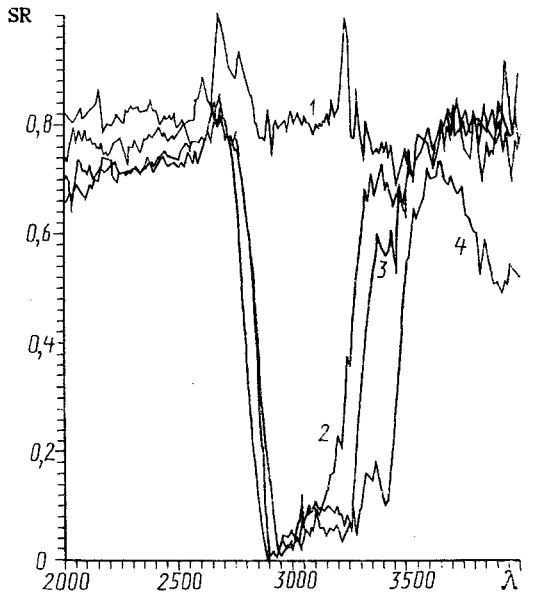

Fig. 4. Reduced spectral reflectance of a metallic mirror coated with layers of water cryocondensate with different thickness on the wavelength of incident radiation (nm) in the near-IR region: 1) clean mirror; 2) r = 0.6 μm; 3) r = 1.2 μm; 4) r = 6.0 μm.

NOTATION

λ, wavelength; m, order of interference; n, indesx of refraction; α, angle of incidence; r, thickness; t, time; ρ, density; M, mass; P, pressure; μ, molecular weight; T, temperature; S, area; and, SR, spectral reflectance.

LITERATURE CITED

1. B. Wood, A. Smith, J. Roux, and B. Zeiber, Raket. Tekh. Kosm., 9, No. 9, 213-221 (1971).
2. B. Wood and A. Smith, Raket. Tekh. Kosm., 16, No. 7, 171-177 (1968).
3. B. Wood, A. Smith, J. Roux, and B. Zeiber, Raket. Tekh. Kosm., 9, No. 7, 155-164 (1971).
4. W. Frost (ed.), Heat Transfer at Low Temperatures, Moscow (1977), pp. 330-345
5. W. Schulse, D. M. Kolb, and G. Klipping, The Density of Cryopumped Gases, Fritz-Haber Institute (1975), pp. 16-110.
6. A. Smith, K. Tempelmeyer, P. Mueller, and B. Wood, Raket. Tekh. Kosm., 7, No. 12, 106-114 (1968).
7. K. Tempelmeyer and D. Mills, J. Appl. Phys., 39, No. 5, 2968-2969 (1968).
8. L. G. Dowell and A. R. Rinfret, Nature, 188, 1144-1148 (1960).
9. A. G. Karpushin and A. S. Drobyshev, Hydroaerodynamics and Diffusion [in Russian], Alma-Ata (1982), pp. 24-31.
10. G. T. Butorin and V. P. Skripov, Thermal Physics [in Russian], Sverdlovsk (1971), pp. 41-47.
11. V. P. Skripov, Thermal Physics and Thermodynamics [in Russian], Sverdlovsk (1974), pp. 41-47.